Process Repeatability in Volume Manufacturing of Nanostructures Utilizing Nanoimprint Lithography

Bradley R Williams, Jim Pierce, Kevin Black, Michael Black, Daniel Bacon-Brown, Rumyana V. Petrova
Moxtek, 452 West 1260 North, Orem, UT 84057;

ABSTRACT

Nanoimprint Lithography (NIL) has demonstrated its value in manufacturing nanostructures with extremely tight tolerances for the optics industry. Processing NIL of single samples in the lab has been completed for decades in industry and academia. There are some obstacles to overcome when scaling up from a representative sample to full wafer, and then again with wafer to wafer to achieve uniformity for many wafers in a row. In this paper, we discuss the process repeatability of manufacturing nanostructures starting from basic lines and spacing through various other periodic and meta structures. Demonstrating the manufacturing capability using NIL for pattering also includes the other related process steps such as thin films and etching. We discuss key metrology, process control characterization, and process stability which include thin film Refractive Index (RI) uniformity, master to print replication uniformity, and post etch structural Critical Dimensions (CD) uniformity. Moxtek's NIL process has achieved 1.0nm σ on line width at 45nm. This precision of replication includes all variation introduced from multiple stamps, wafer to wafer prints, and multiple sites within the wafer. This level of process control at the masking layer needs to be maintained for the finished structure.

Keywords: NIL, CD, Volume Manufacturing, Process Variability, SCIL, Wire Grid Polarizer, Pillar, Metalens

1. INTRODUCTION

Nanoimprint Lithography (NIL) has been a well-known process in industry and academia for decades. Many different forms of NIL are in use today including roll to roll, wafer level printing, and jet and flash [1]. Defects in NIL processing is a significant challenge to overcome before it can become well utilized in semiconductor manufacturing [2]. In optics manufacturing, the acceptable levels of defects are not as stringent as semiconductors manufacturers and make NIL a viable patterning option. Moxtek has manufactured Wire Grid Polarizers (WGP) for many years with significant process and market understanding. Moving to improve manufacturing capability Moxtek has installed and released for production an AUTOSCIL200 NIL system. This process was qualified in volume manufacturing of WGP on 200mm wafers.

Capitalizing on the benefits observed during the integration of NIL into WGP production, other structures were also evaluated. It was demonstrated that NIL is particularly effective in reproducing structures that would be rather challenging for conventional lithography processes [3]. A few structures of interest included pillars, slanted gratings, and multilevel structures. These structures are used in many applications including flat lenses and waveguides [4][5]. Nearly all the published work incorporating these nanostructures is with small areas that can be patterned with E-Beam lithography. The next step is to demonstrate volume manufacturability. When this is done NIL will become a key to making optical applications a reality.

2. DISCUSSION

Constructing Diffractive Optics Elements (DOEs) has three main building blocks. The first building block is identifying material with a high Refractive Index (RI) in relation to air and the glass substrate. One important consideration for materials is its ability to be etched. The designed nanostructure needs to be etched into the high RI material. The second building block is the ability to pattern a large area with the designed nanostructures. This is where NIL provides some advantages compared to standard lithography options. The third building block is etching the nano pattern into the high index material. This etching can be challenging as some high RI materials are rather etch-resistant such as TiO_2. Another challenge is handling the aspect ratios of the designed structures which can be up to 9:1 or more.

2.1 High Index Thin Films

High RI thin film layers are needed to build DOEs. Film layers can be as thick as 1.0um but since these are optical devices the RI needs to be uniform through the full thickness of the layer. To evaluate Moxtek's thin films deposition capability, two high RI materials were selected, TiO_2 and Nb_2O_5. These films were deposited at varying thickness and measured for the optical properties. As shown in Figure 1, for both materials the RI is consistent over each film thickness from 100nm up to 1000nm (700nm for Nb2O5). The extinction coefficient is very low for both films.

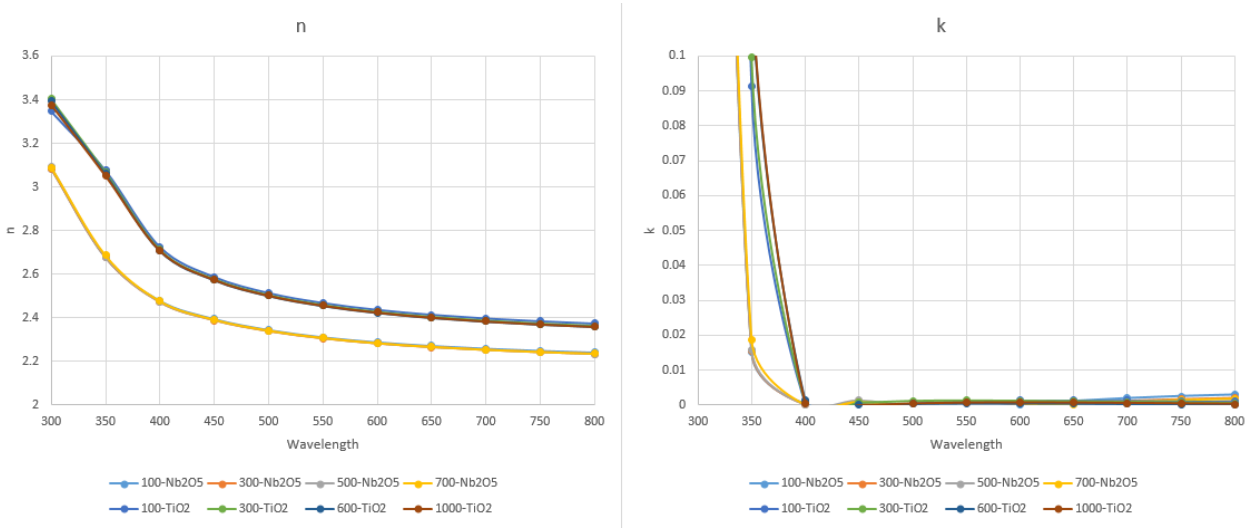

Figure 1. The refractive index and extinction coefficient are displayed for TiO_2 and Nb_2O_5 at varying thicknesses.

From previous work, we know that etching TiO_2 has some processing challenges. Also, TiO_2 film can have tendencies to be less consistent due to oxygen vacancies [6]. Based on the complications of using $Ti0_2$, Nb_2O_5 was selected to demonstrate the capability of NIL.

2.2 Nanoimprint Lithography Process

AutoSCIL 200 nanoimprint system was installed into a WGP production line at Moxtek. NIL process stability has been established for line space patterns measured by an Atomic Force Microscope (AFM). The NIL process has Statistical Process Control (SPC) that monitors the printed line structure for line width and print height. As the AFM scans an image of a set area including multiple lines the line width and print height is an average across the scan area. The recorded SPC values include multiple sites on a wafer. The function of SPC is a continuous monitor that captures multiple stamps and identifies any increase in variability. This data set includes the variation observed from within wafer, wafer to wafer, and stamp to stamp. A secondary variation source is from the AFM probe tip. Systems are in place to identify probe tip variation and remove it from the data set.

Line space imprint repeatability has a standard deviation of 1.0nm on a nominal line width of 45nm. This print repeatability is represented in Figure 2. The data set includes six different stamps from a single master. Prints per stamp were up to 275 on a stamp in the shown data set. Basic stamp life was demonstrated during the original installation up to 700 prints per stamp measured by WGP optical performance.

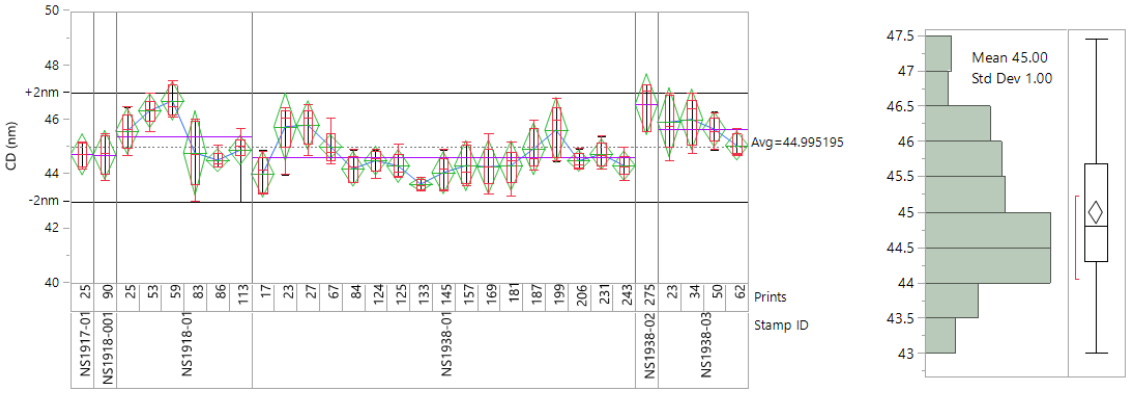

Figure 2. Sample of line width SPC data set that is from the same master. Replication shows six different stamps and print counts up to 275 wafers on a stamp. Each grouping is a wafer measured at five locations.

The next structure to evaluate imprint process performance is 144nm pitch pillars in a square pattern. To measure reasonable values of pillar width, print height, circularity, and slope, the AFM scan size and resolution were increased which also significantly increased scan time. Therefore pillars were only measured on three sites per wafer. Pillar analysis, which helped us obtain critical metrics, was performed using PIL_AFM, software provided by Nanometrisis P.C. The size of each scan was set to capture 12 full pillars per scan for analysis.

Setting up a systematic measure method for pillars so that it will fit well into an SPC system is more challenging than for line/space patterns. Much time was devoted to ensuring the AFM measure and analysis methods were repeatable. This limited the amount of process data available by the time of this report. We were able to produce a data set with five measurements. As the process continues to run we will have data from multiple wafers and multiple stamps.

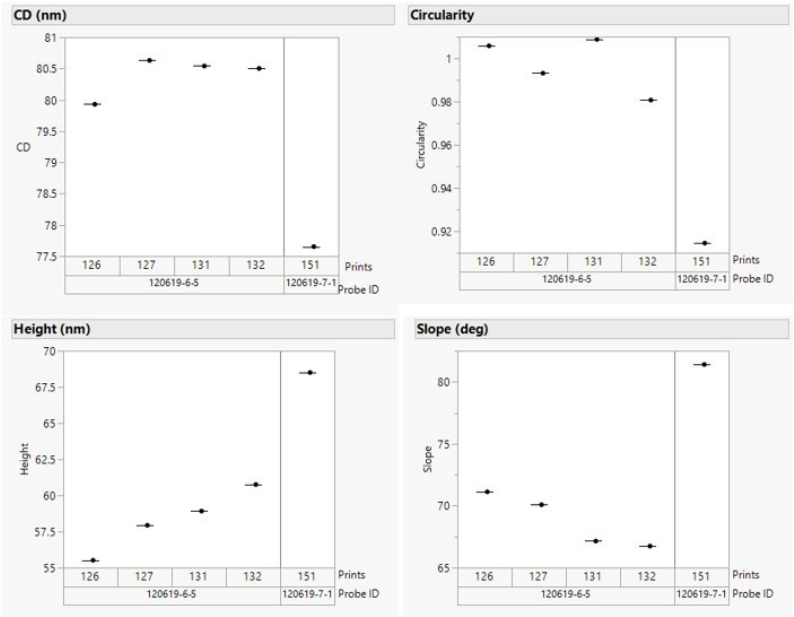

Figure 3. Five printed wafers show pillar dimensions. Four wafers were measured with the same AFM probe tip and one wafer measured with a different AFM probe tip.

The first observation is that different AFM probe tips show far more variation than the print to print variation (see Figure 3). Improved probe tip calibration is needed for improving pillar signal to noise measurements. However, when using the same probe tip, the pillar CD variation is ± 0.5nm on the first set of prints. Future investigations will include characterization of multiple stamps. Testing shows a rather uniform print height ± 2.6nm and the slope appears to also have minimal variation ± 2.2degrees. In order to understand variation and SPC control the AFM recipe must stay

unchanged. With this in mind changes in AFM recipe setup such as; scan size, scan direction, probe tip force, and many more can have a large impact on measured output. This provides relative values around a mean and the variation between samples in a continuous process.

Finally, in evaluating pillar print performance we looked at the difference between master and print. As shown in Table 1 the printed CD, height, and slope are less than the master which is expected, but the round shape of the printed pillar matches the master very well.

Table 1. Average pillar dimensions for four printed wafers compared to the dimensions of the master wafer as measured on AFM and post etch measured wafer.

	Mean CD (nm)	Circularity (CD_x/CD_y)	Mean Height (nm)	Mean Slope (deg)
4 Printed wafers on the same AFM probe tip	80.40	0.997	58.28	68.78
Master wafer	85.85	0.978	67.34	74.46
Post etch of 100nm Nb2O5 layer with etch mask remaining	114.54	1.010	186.73	83.47

2.3 High Aspect Ratio Etch

After the structure is replicated into a pattern, that pattern then needs to be etched into the high RI layer. Depending on the application and the RI of the material chosen, the etch depth required could be up to and beyond 700nm. For this, we evaluated etching pillars into Nb_2O_5. First, we etched a 100nm layer so we could evaluate etch bias from printed to post etch critical dimensions. In order to compare the pillars with the previously printed wafers which were measured on the AFM, an etched structure was needed that can also be measured on the AFM using the same recipe as described above. Any etched pillars much deeper than 100nm would cause issues with the AFM setup and probe tip.

The etch bias is rather large for the current etch process at +34nm as shown in Table 1. Continued work is in progress to optimize the etch process and minimize the bias. Even with this increase in pillar CD we have completed etches 750nm deep. Future work is ongoing to test various pillar size and pattern. As shown in Figure 4 etch depths up to 750nm have been demonstrated with a very dense pillar structure.

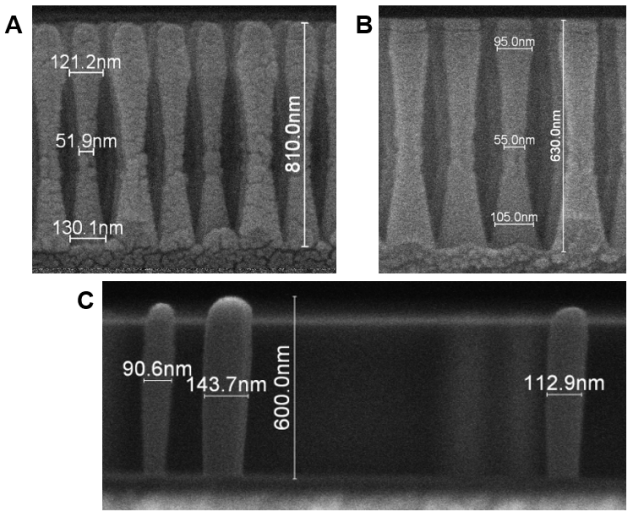

Figure 4. A) Dense post etch 750nm deep Nb_2O_5. B) Dense post clean 610nm deep Nb_2O_5 C) Isolated various CD post etch 600nm Nb_2O_5

3. CONCLUSIONS

NIL has shown repeatable pattern replication across a 200mm wafer for line/space patterns with CD σ = 1.0nm on 45nm line. Also, pillar prints across a 200mm wafer show initial results that indicate CD uniformity ± 1nm or less on an 80nm pillar. While future work over multiple stamps is ongoing, the pillar data is from a small sample on a single stamp.. The ability to manufacture pillars in a high index material across a full 200mm wafer in high volume proves that the flat metalens application is very possible [7],by using NIL this process can become less costly.

4. REFERENCES

[1] T. Higashiki, T. Nakasugi, and I. Yoneda, "Nanoimprint lithography for semiconductor devices and future patterning innovation," in *Alternative Lithographic Technologies III*, Mar. 2011, vol. 7970, p. 797003, doi: 10.1117/12.882940.

[2] M. Hatano *et al.*, "NIL defect performance toward high volume mass production," San Jose, California, United States, Mar. 2016, p. 97770B, doi: 10.1117/12.2218972.

[3] H. Schift, "Nanoimprint lithography: 2D or not 2D? A review," *Appl. Phys. A*, vol. 121, Apr. 2015, doi: 10.1007/s00339-015-9106-3.

[4] B. Li, W. Piyawattanametha, and Z. Qiu, "Metalens-Based Miniaturized Optical Systems," *Micromachines*, vol. 10, no. 5, Art. no. 5, May 2019, doi: 10.3390/mi10050310.

[5] J. D. Waldern, R. Morad, and M. M. Popovich, "Waveguide Manufacturing for AR Displays, Past, Present and Future," in *Frontiers in Optics / Laser Science (2018), paper FW5A.1*, Sep. 2018, p. FW5A.1, doi: 10.1364/FIO.2018.FW5A.1.

[6] X. Pan, M.-Q. Yang, X. Fu, N. Zhang, and Y.-J. Xu, "Defective TiO2 with oxygen vacancies: Synthesis, properties and photocatalytic applications," *Nanoscale*, vol. 5, Mar. 2013, doi: 10.1039/c3nr00476g.

[7] J.-S. Park *et al.*, "All-Glass, Large Metalens at Visible Wavelength Using Deep-Ultraviolet Projection Lithography," *Nano Lett.*, vol. 19, no. 12, pp. 8673–8682, Dec. 2019, doi: 10.1021/acs.nanolett.9b03333.